Electronic Supplementary Information

Homogeneous versus Heterogeneous Catalysis in Cu_2O-nanoparticle-catalyzed C-C Coupling Reactions

Ravi Teja Addanki Tirumala[a], Andishaeh P. Dadgar[a], Farshid Mohammadparast[a], Sundaram Bhardwaj Ramakrishnan[a], Tong Mou[b], Bin Wang[b], Marimuthu Andiappan[a]*

[a.] *School of Chemical Engineering, Oklahoma State University, Stillwater, OK, USA*
[b.] *School of Chemical, Biological and Materials Engineering, The University of Oklahoma, Norman, OK, USA*

This file includes

Materials and Methods

Figs. S1 to S20

Reference Cited for Electronic Supplementary Information

*Corresponding author, Email: mari.andiappan@okstate.edu

I. **Experimental Section**

Cu_2O nanoparticles Preparation and Characterization

Cu_2O nanoparticles (NPs) were prepared using the water-in-oil microemulsion synthesis technique.[1] The technique uses n-heptane (99% Fisher Cat. No. AC447070025), polyethylene glycol-dodecyl ether (average Mn ~362, Sigma-Aldrich Cat. No. 235989), copper nitrate (99.999%, Sigma-Aldrich Cat. No. 229636), and hydrazine (98% Sigma-Aldrich Cat. No. 215155) as the continuous oil phase, surfactant, precursor and reducing agent, respectively. The reducing agent to precursor molar ratio was 10 and water to surfactant molar ratio was 30. Concisely, an aqueous solution of copper nitrate (0.1 M) was added to a mixture of n-heptane and surfactant (16.54 wt%) under stirring. A one molar aqueous solution of hydrazine was dripped in drop by drop into the synthesis mixture under stirring. The mixture was kept under continuous stirring at room temperature for a total synthesis time of 12 hours. At the end of the synthesis, the solution transferred into the centrifuge tube where acetone was added to break the emulsion. The nanoparticles were separated from the remaining solution through centrifugation at 3750 rpm for 20 minutes. The nanoparticles were washed four times with acetone to remove the surfactant and separated from the solution via centrifugation and used as the catalyst for the subsequent coupling reactions. The representative TEM image of as-prepared Cu_2O nanoparticles (diameter=34 ± 4 nm) is shown in Fig. S1. TEM images were taken using a JEOL JEM-2100. The TEM is equipped with a LaB6 gun and accelerating voltage of 200 kV. The signatures of Cu_2O were confirmed using the X-ray diffraction (XRD) pattern and the UV-vis extinction spectrum shown in Fig. S2 and Fig. S3, respectively. XRD pattern were acquired using a Philips X-Ray diffractometer (Phillips PW 3710 mpd, PW2233/20 X-Ray tube, Copper tube detector – wavelength - 1.5418 Angstroms), operating at 45 KW, 40 mA. All UV-Vis extinction spectra reported here were taken using an Agilent Cary 60 Spectrophotometer. The extinction spectrum shown in Fig. S3 is consistent with the band gap (i.e., 2.1 eV) of Cu_2O.[1]

C-C Coupling Reaction Conditions and Characterization

Cu_2O NPs were synthesized using the microemulsion synthesis technique. The NPs were suspended in dimethylformamide (DMF, 15 mL) before starting the reaction (34.08 mg, 0.598 mmol). The suspended NPs were added to a 25 mL round bottom flask (RBF) connected with a condenser and a thermocouple for temperature control. Air or nitrogen (purity-99.999%) was continuously flowed through the RBF to maintain the respective gas environment in the oxidative homocoupling reaction (OHR) and Sonogashira cross-coupling reaction (SCR). Potassium carbonate (K_2CO_3) was weighed out (207 mg, 1.64 mmol) and added while stirring the nanoparticles and DMF. For cross-coupling reactions, Iodobenzene (IB, 0.91 mmol) was added while still stirring. The mixture was then heated for ~15 minutes to reach 110 ^oC for homocoupling and 147 ^oC for cross-coupling reaction. At this point, phenylacetylene (PA, 0.91 mmol) was added, and the reaction was started. The reaction mixture was sampled at frequent time intervals to quantify the reaction conversion and product selectivity using GC-MS (Shimadzu QP2010SE). The homocoupling of PA into diphenyladiacetylene (DPDA) was observed only in the presence of oxygen. A Shimadzu C184-E037A GC Column (Phase: SH-Rxi™-5Sil MS Column, Length-30 m; ID – 25 mm; df – 0.25 µm) was used for gas chromatography. The column had an operating temperature range of -60 °C to 320/350 °C. Peak detection and integration were handled by the software provided by the Shimadzu Corporation. Identification was verified using NIST spectral libraries with matching higher than 95%. No smoothing was used to process the samples to ensure accurate peak identification and quantification. The calibration curves were built independently using area versus concentration response from prepared reference samples.

The conversion was calculated based on the equation shown below:

$$Conversion\ (X, \%) = \frac{C_{A0} - C_A}{C_{A0}} * 100$$

where C_{A0} is the initial concentration (in mmol) of reactant (i.e., PA) and C_A is the concentration at any time, t.

The product selectivity for SCR was calculated based on the equation shown below:

$$Selectivity\ (DPA\ or\ DPDA, \%) = \frac{C_{DPA\ or\ DPDA}}{C_{DPA} + C_{DPDA}} * 100$$

where C_{DPA} and C_{DPDA} are the concentration (in mmol) of the desired cross-coupling product (diphenylacetylene, DPA) and the undesired homocoupling product (diphenyldiacetylene, DPDA), respectively.

The conversion of PA at a reaction temperature of 147 ^oC under reflux and nitrogen flow (99.999% purity) as a function of reaction time for SCR between PA and IB under the base and base-free conditions are shown in Fig. S4 and Fig. S5, respectively. The product selectivity towards DPA and DPDA under the respective conditions are shown in Fig. S6 and Fig. S7. We also carried out SCR between PA and bromobenzene (BB). The PA conversion of this reaction under the base and base-free conditions are shown in Fig. S15 and Fig. S16, respectively. The product selectivity observed towards DPA and DPDA under SCR between PA and BB are shown in Fig. S17 and Fig. S18. The UV-Vis extinction spectra of the reaction mixture of the SCR between PA and BB under the base-and base-free conditions are shown in Fig. S19 and Fig. S20, respectively. Similar to the results observed for SCR between PA and IB, the results of SCR between PA and BB in Fig. S15-20 show that (a) longer reaction completion time is required under base-free conditions, (b) similar product selectivity are observed

under base and base-free conditions, and (c) the extinction features of homogenous Cu complexes (centered at ~385 and ~450 nm) are present in the UV-Vis extinction spectra of the reaction mixture only under base-free conditions.

Electrospray ionization mass spectrometry (ESI-MS) spectra of the supernatant solution of the reaction mixture were collected on LTQ Orbitrap system with an ESI source. The spray voltage was set at 5.0 kV with 15.0 mL/min sample flow rate. To achieve proper spraying conditions, the sample was prepared by mixing 1 mL of sample with 1 mL of a mixture of 18 mL dichloromethane, 2 mL Acetone, 400 µL DI water. The sample was sprayed with nitrogen as the sheath and auxiliary gas. Fig. S10 shows the representative HR-ESI-MS spectrum measured in negative spray mode for the supernatant solution of the reaction mixture collected from SCR in the presence of the base. The signals from this ESI-MS spectrum in the m/z range of 281-284 and 299-302 match the predicted isotope distributions of copper complexes, $[CuO(C_8H_5)_2]^-$ and $[CuO(C_8H_5)_2H_2O]^-$, respectively, shown in Fig. S11a-b. The combination of ESI-MS, UV-Vis extinction spectroscopy and DFT results confirm that in the presence of base, the homogeneous Cu complex, $[CuO(C_8H_5)_2]^-$, is the common catalytic species formed under homo-coupling as well as cross-coupling conditions via PA-induced leaching of Cu_2O NPs surface atoms. The reactor study results using GC-MS analysis also show that this homogeneous Cu complex can efficiently catalyze both reactions: (i) OHR with ~100% selectivity towards the desired homocoupling product, DPDA when the reaction is performed under air flow at a reaction temperature of 110 °C, and (ii) SCR with >95% selectivity towards the desired cross-coupling product, DPA at 147 °C (under reflux) and under nitrogen (99.999% purity) flow.

Flame-atomic absorption spectroscopy (FAAS) analysis of the supernatant solution of the reaction mixture was performed on a Varian Fast Sequential AA240FS – Flame Spectrophotometer. For the quantification of Cu content, the calibration curve was built using area versus concentration response using standard samples with known concentrations of copper nitrate. A hollow cathode lamp (324.7 nm) for the element copper is used with the slit width 0.5 mm. The flame temperature was 2000 °C and was produced using acetylene and air as the fuel mixture. The detection limit of the instrument for Cu is 100 parts per billion (ppb).

II. DENSITY-FUNCTIONAL THEORY (DFT) CALCULATIONS

DFT computations were carried out using Vienna ab initio simulation package (VASP).[2] The projector-augmented wave (PAW) approach was used to describe the interaction between ion cores and valence electrons.[3] For the structural optimization, the exchange and correlation energy was represented using the Perdew-Burke-Ernzerhof (PBE) functional of the generalized gradient approximation (GGA).[4] The DFT-D3 semi-empirical van der Waals (vdW) correction proposed by Grimme has been taken into account in all calculations.[5,6] An implicit solvation model, VASPsol [7,8], was employed in all the calculations, to account for liquid solvent environments. The Brillouin zone was sampled by a k-point mesh of 1 × 1 × 1 for geometry optimizations and optical property calculations. The energies of complex molecules in vacuum were computed using a 20 × 20 × 20 Å unit cell. An extra electron was manually placed at LUMO (lowest unoccupied molecular orbital) of the molecule to include the negative charge. The cutoff energy was set at 400 eV. The structures were relaxed until the atomic force is smaller than 0.02 eV/Å, and the energy tolerance was set to 10-5 eV. All the ion relaxations were performed using a Gaussian smearing with a width of 0.2 eV, and 0.4 eV for optical absorption spectra calculations, respectively. The OPTICS code of Furthmüller was employed to compute the imaginary part of the dielectric constant and hence the absorption spectra.[9] The imaginary part of the dielectric constant, which is proportional to the optical absorption, is determined by the summation of empty states in the conduction band that can be compared to the features of the experimental spectra. The DFT-predicted structures of the proposed homogeneous Cu complexes, $[CuO(C_8H_5)_2]^-$ and $[CuO(C_8H_5)_2H_2O]^-$, are shown in Fig. S11d and Fig. S11e, respectively.

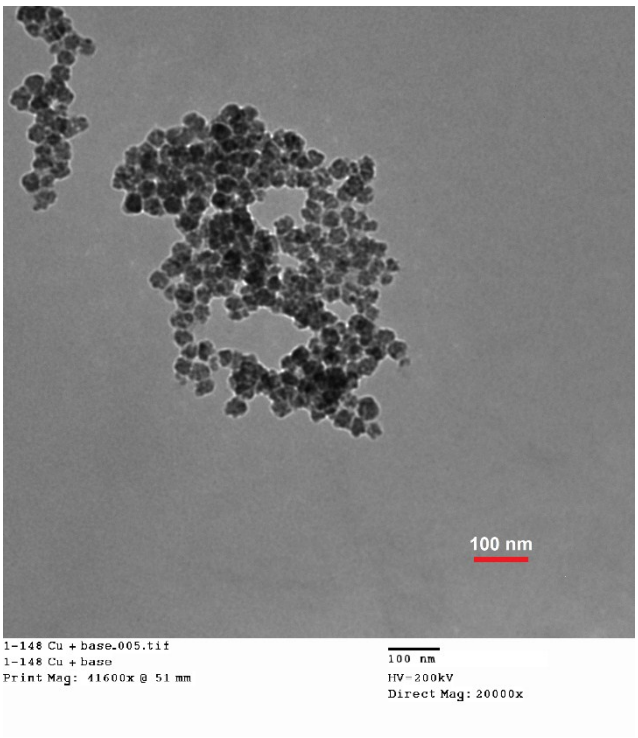

Fig. S1. A representative TEM image of the Cu_2O nanoparticles (diameter = 34 ± 4 nm).

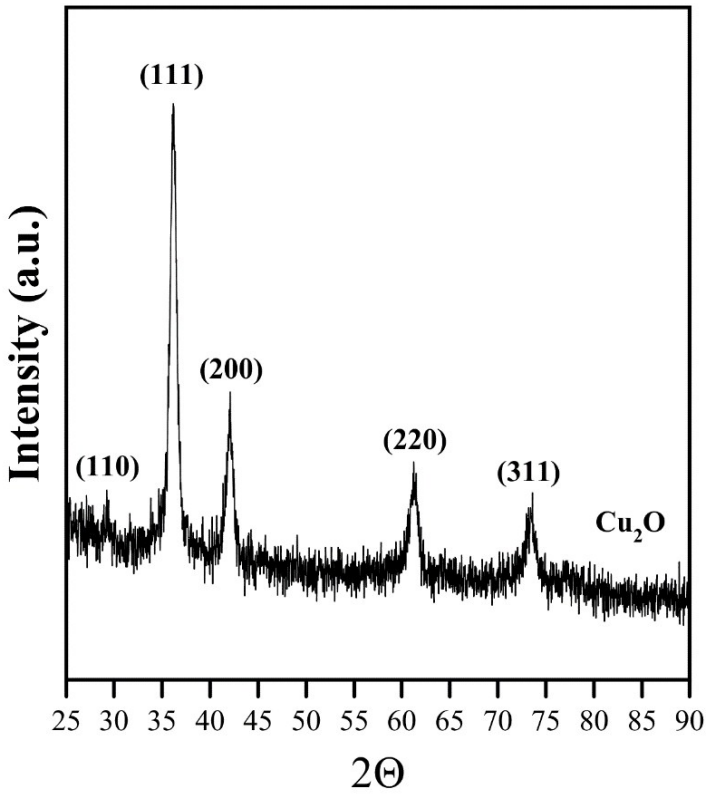

Fig. S2. The X-Ray diffraction pattern of the Cu_2O nanoparticles.

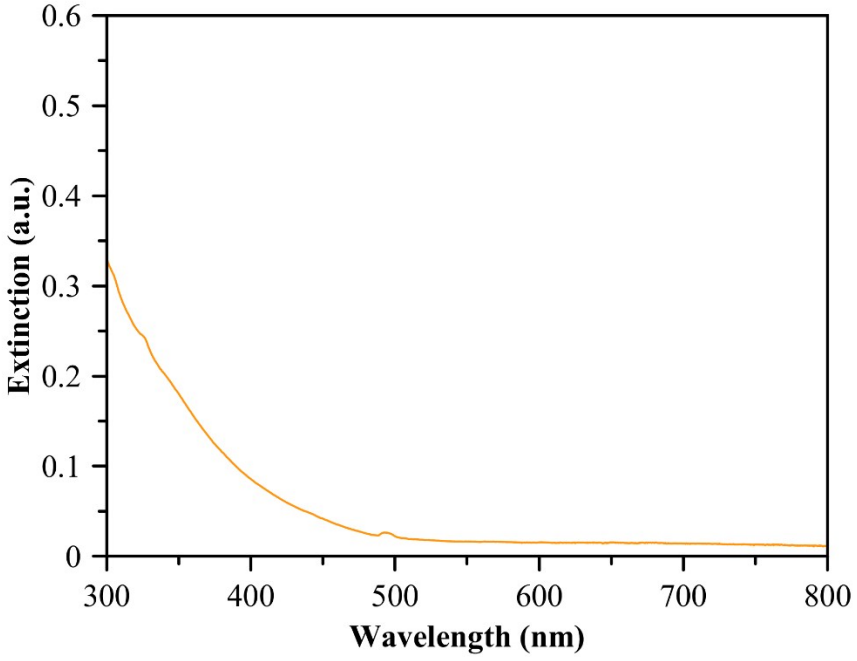

Fig. S3. The UV-Vis extinction spectrum of the Cu_2O nanoparticles.

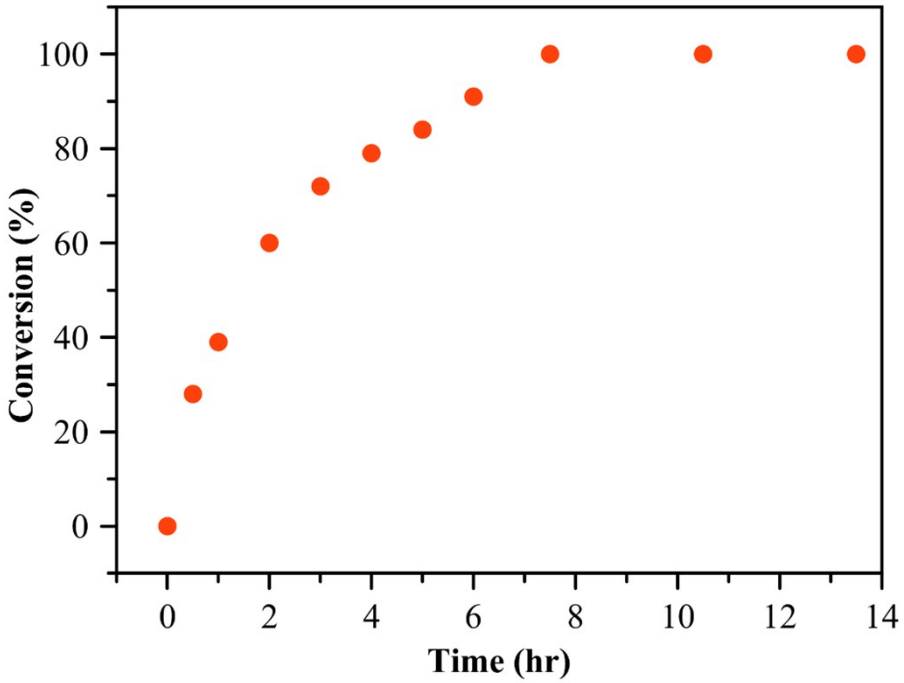

Fig. S4. Conversion as a function of Reaction Time for SCR at 147 °C (under reflux) in the presence of the base.

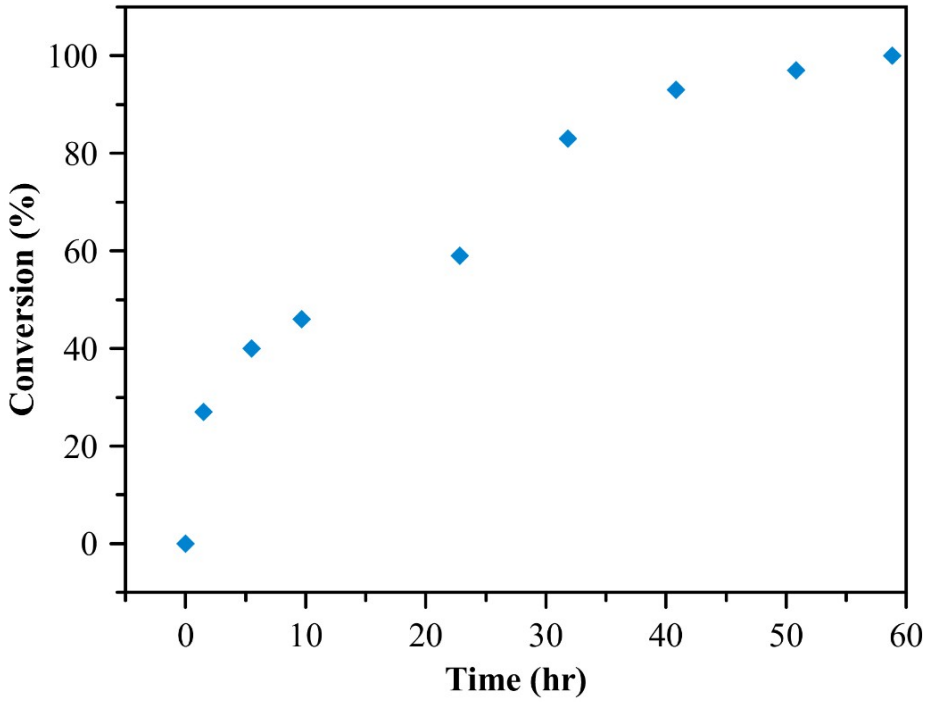

Fig. S5. Conversion as a function of Reaction Time for SCR at 147 °C (under reflux) in the absence of the base.

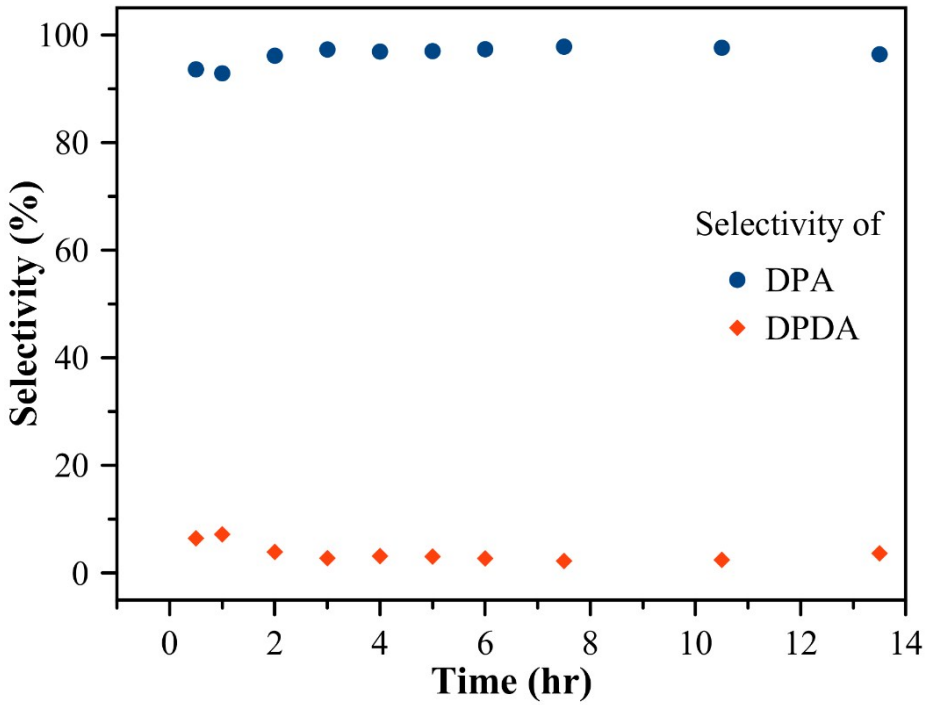

Fig. S6. The cross-coupling and homocoupling products DPA vs DPDA selectivity as a function of reaction time for SCR at 147 °C (under reflux) in the presence of the base.

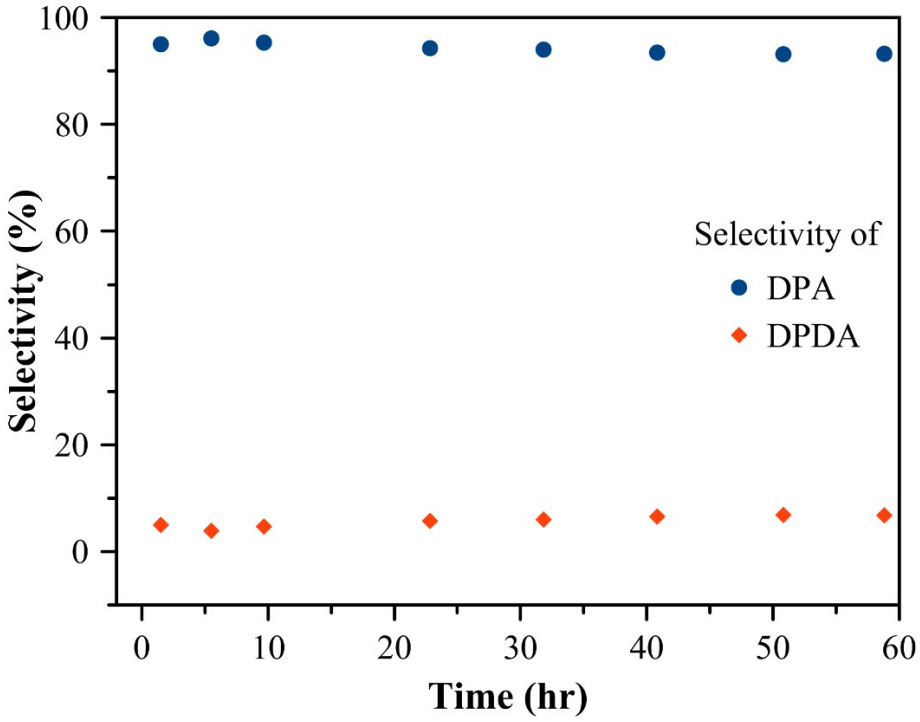

Fig. S7. The cross-coupling and homocoupling products DPA vs DPDA selectivity as a function of reaction time for SCR at 147 °C (under reflux) in the absence of base.

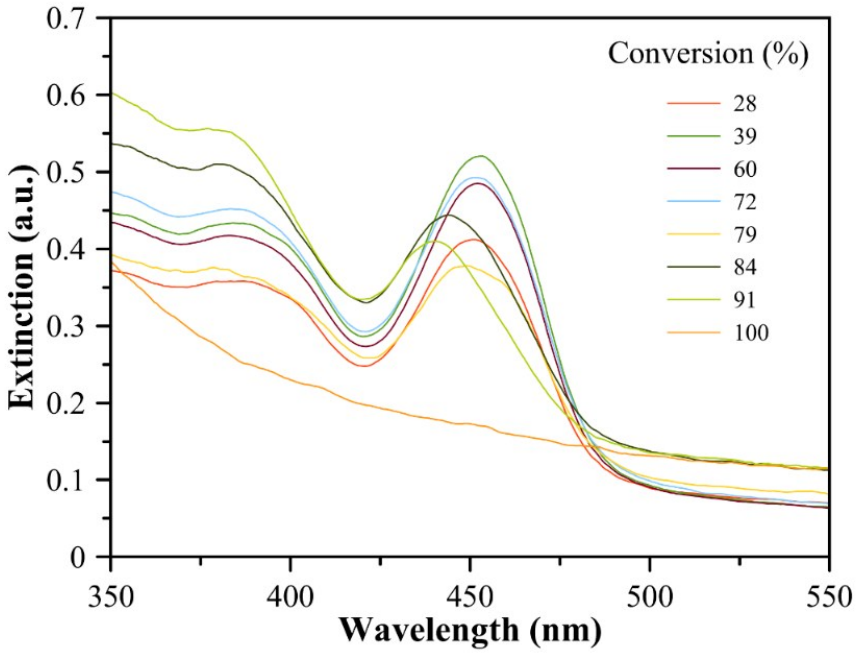

Fig. S8. UV-Vis extinction spectra of reaction mixture measured at different reaction conversions during SCR at 147 °C (under reflux) in the presence of base. The extinction peaks centered at ~385 and ~450 nm in Fig. S8 are due to homogeneous Cu complexes in the reaction solution. These peaks are observed in the reaction solution only when both PA and base are present. We did not observe any leaching or the extinction peaks for the homogeneous Cu complexes when only IB and base were present (in the absence of PA).

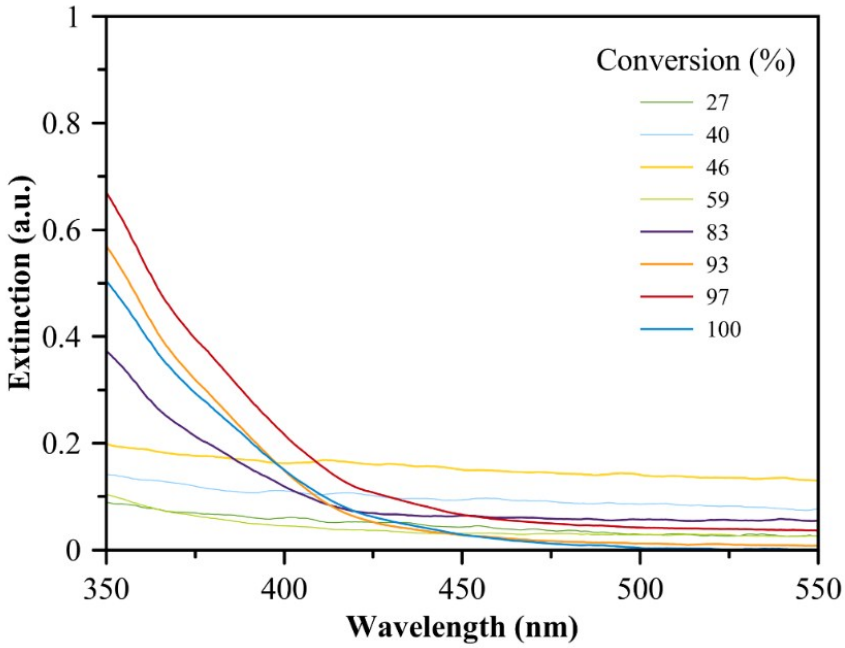

Fig. S9. UV-Vis extinction spectra of reaction mixture measured at different reaction conversions during SCR at 147 °C (under reflux) in the absence of the base. The changes observed in the extinction spectra in Fig. S9 for different conversions are most likely due to the expected change in dielectric constant of the reaction mixture for the respective conversions.

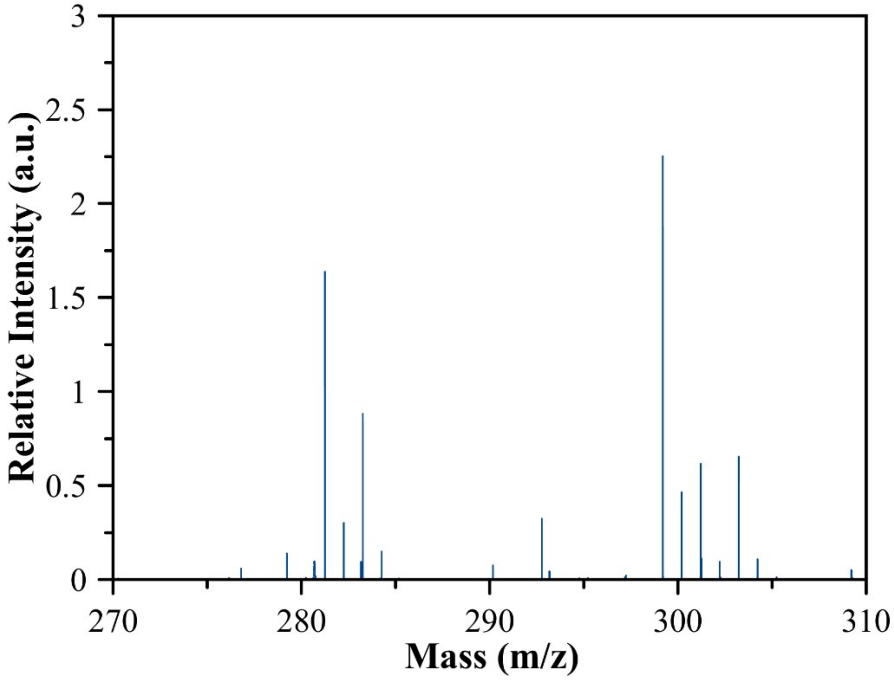

Fig. S10. The HR-ESI-MS spectrum measured in negative spray mode for the supernatant solution of the reaction mixture taken from Cu_2O nanoparticles-catalyzed SCR in the presence of the base.

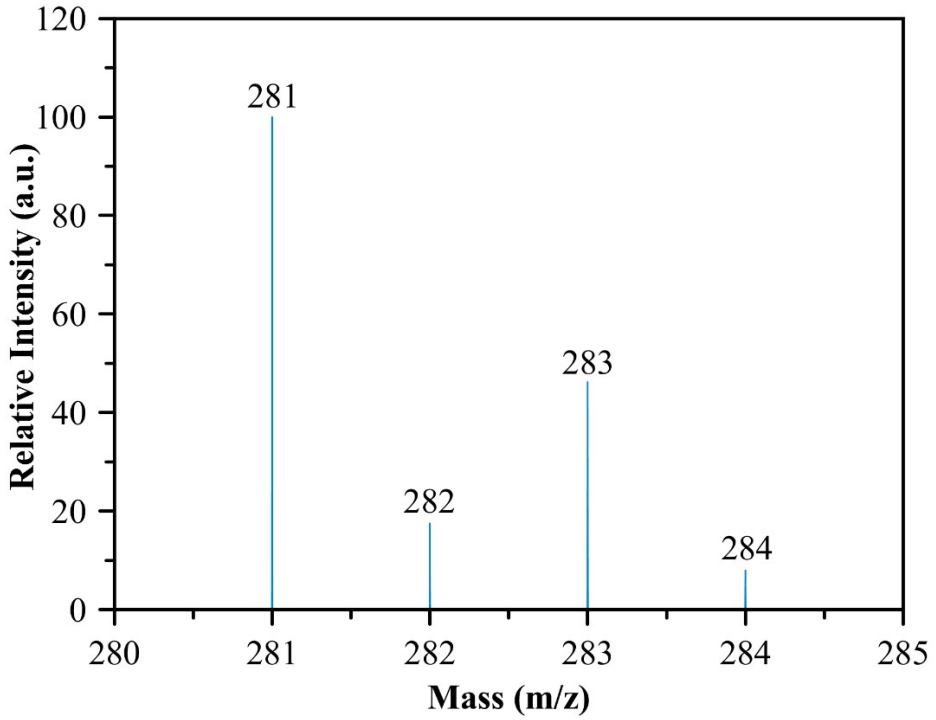

Fig. S11a. Predicted mass spectrum for the proposed copper complex with chemical formula, $[CuO(C_8H_5)_2]^{-}$.[10]

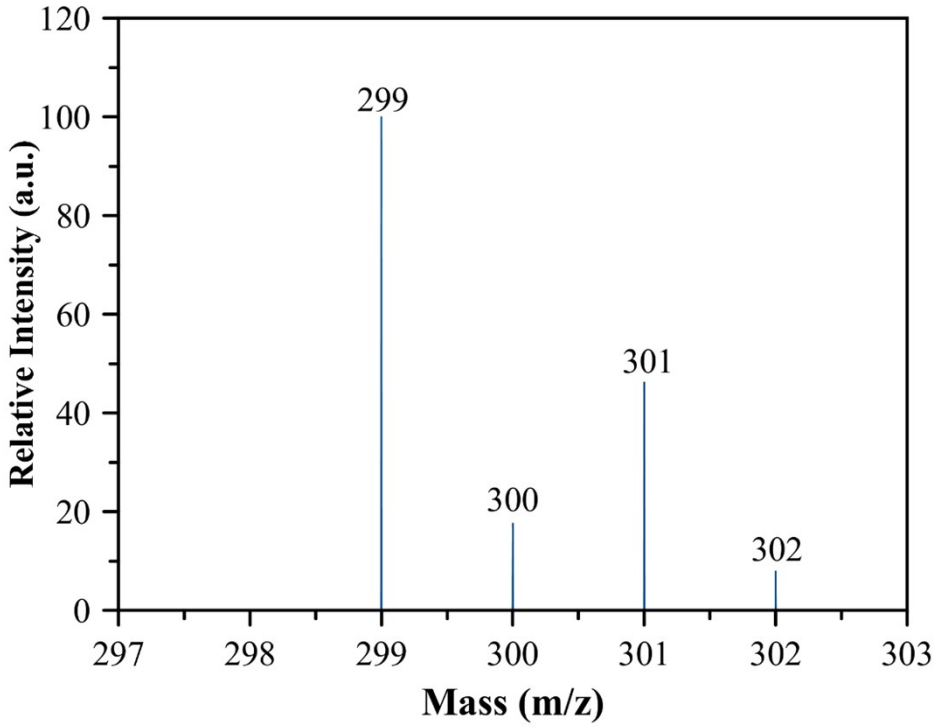

Fig. S11b. Predicted mass spectrum for the proposed copper complex with chemical formula, $[CuO(C_8H_5)_2H_2O]^-$. [10]

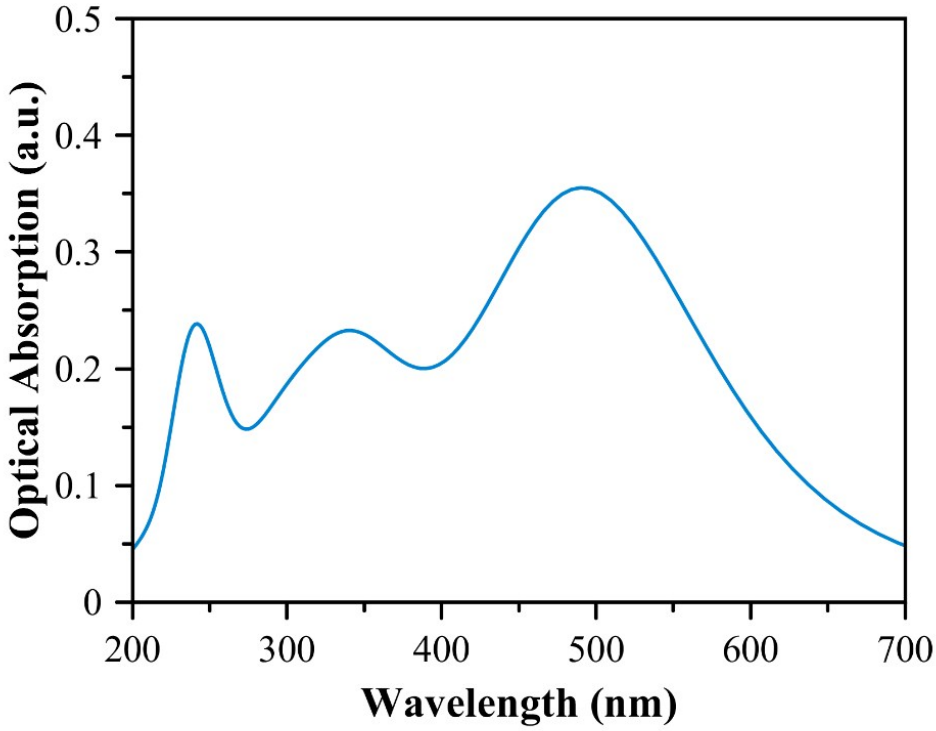

Fig. S11c. DFT calculated optical absorption spectra of homogeneous Cu complex, $[CuO(C_8H_5)_2H_2O]^-$.

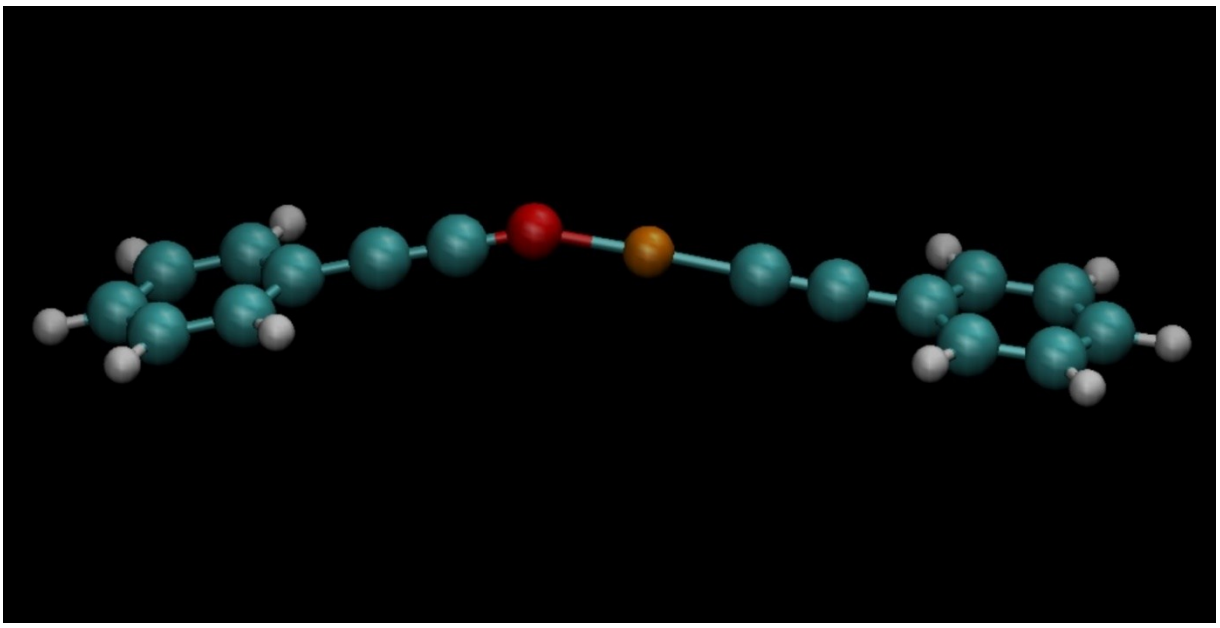

Fig. S11d. DFT-predicted Structure of homogeneous Cu complex, $[CuO(C_8H_5)_2]^-$. Color code: Orange - Copper atom; Red – Oxygen atom; Cyan-Blue – Carbon atom, White – Hydrogen atom.

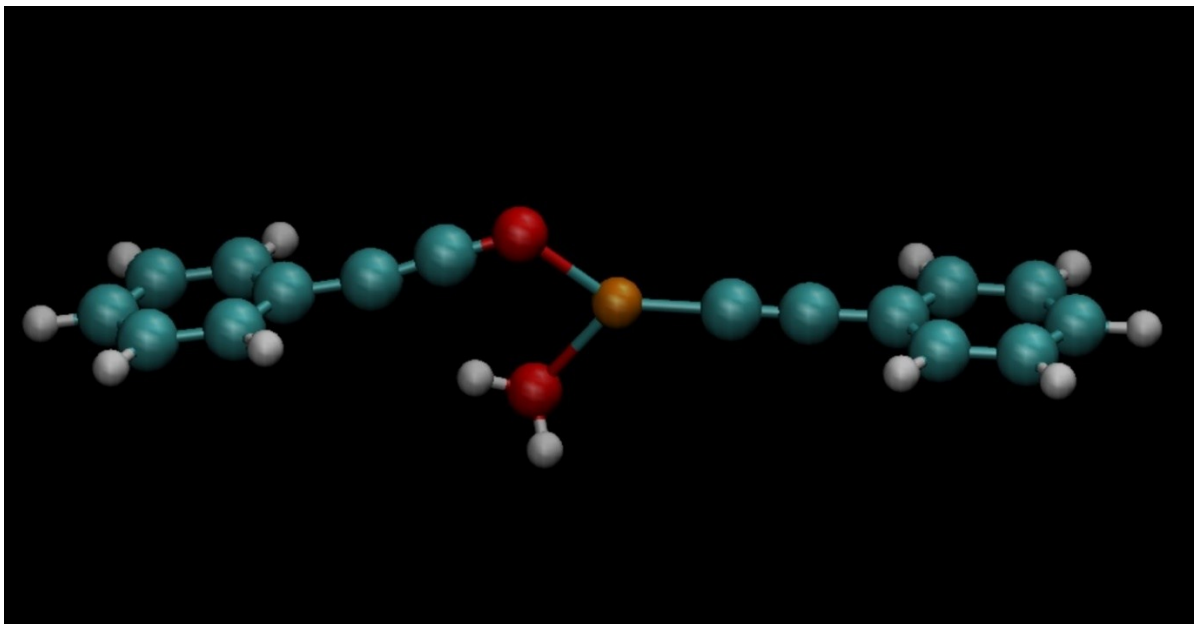

Fig. S11e. DFT-predicted Structure of homogeneous Cu complex, $[CuO(C_8H_5)_2H_2O]^-$. Color code: Orange - Copper atom; Red – Oxygen atom; Cyan-Blue – Carbon atom, White – Hydrogen atom.

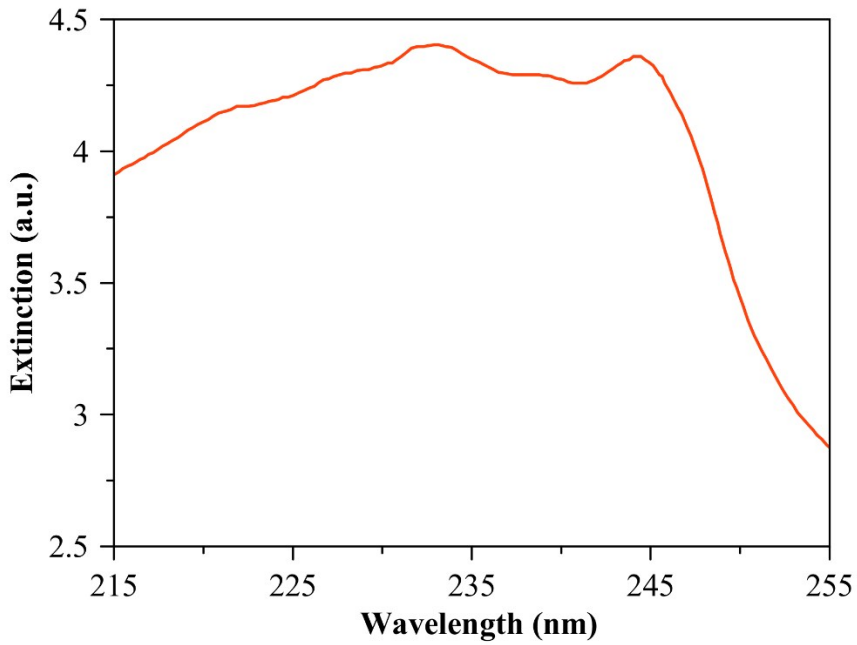

Fig. S12a. UV-Vis extinction spectrum of Phenylacetylene (PA) can be found in the reference.[11]

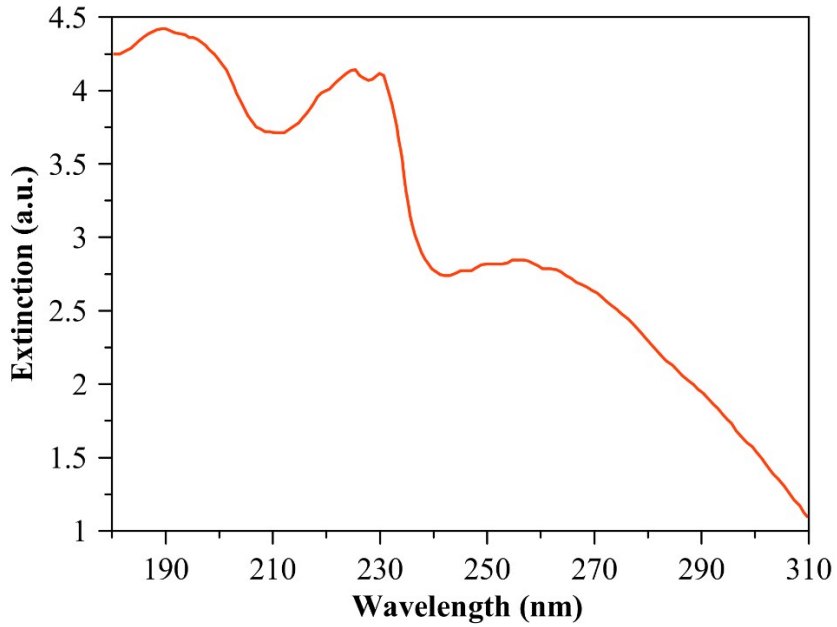

Fig. S12b. UV-Vis extinction spectrum of Iodo-Benzene (IB) can be found in the reference.[12]

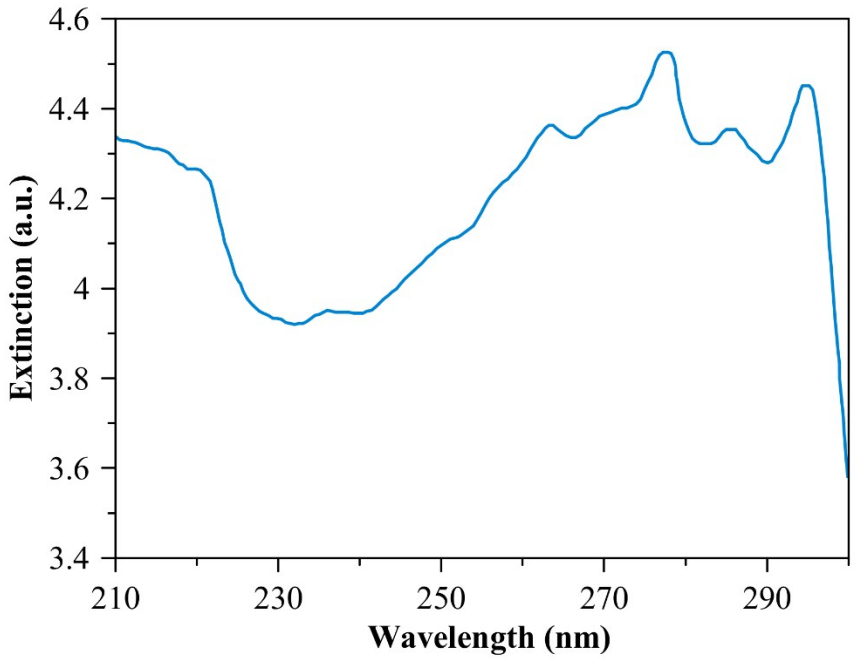

Fig. S12c. UV-Vis extinction spectrum of Di-phenyl Acetylene (DPA) can be found in the reference.[13]

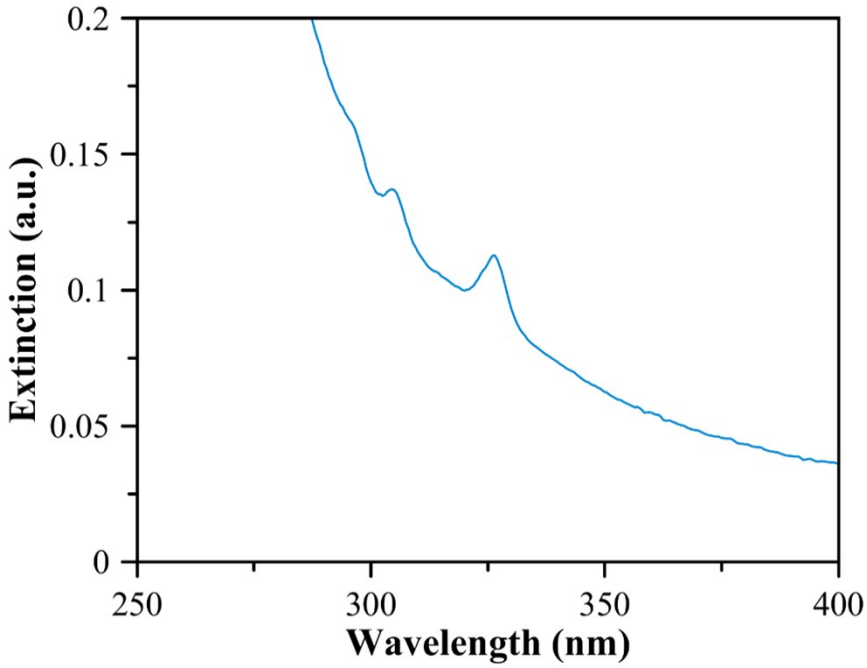

Fig. S12d. UV-Vis extinction spectrum of diphenyldiacetylene (DPDA).

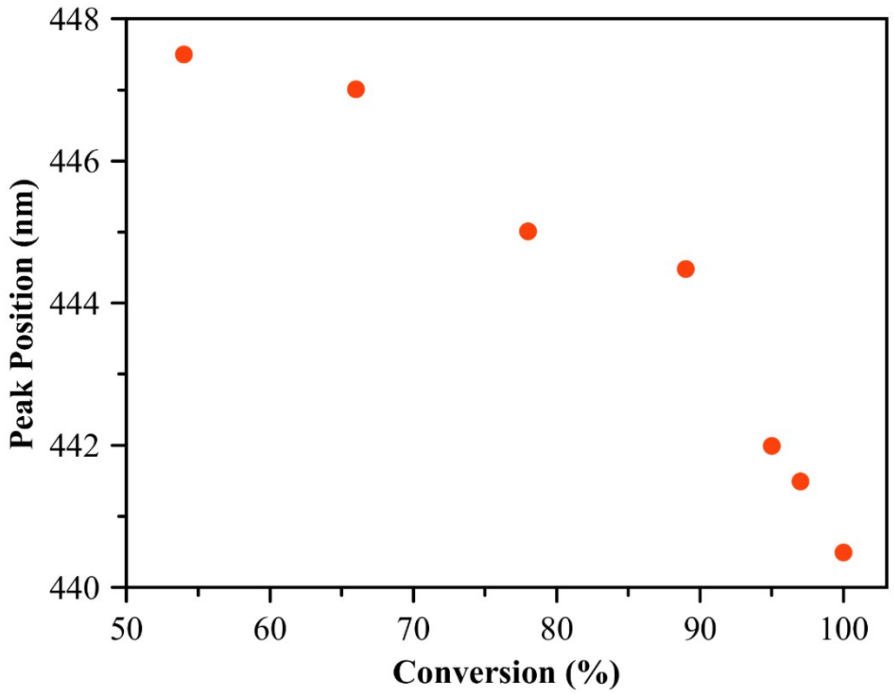

Fig. S13a. Extinction peak position in the 440-450 nm region of the UV-Vis extinction spectrum as a function of PA conversion for OHR in the presence of base.

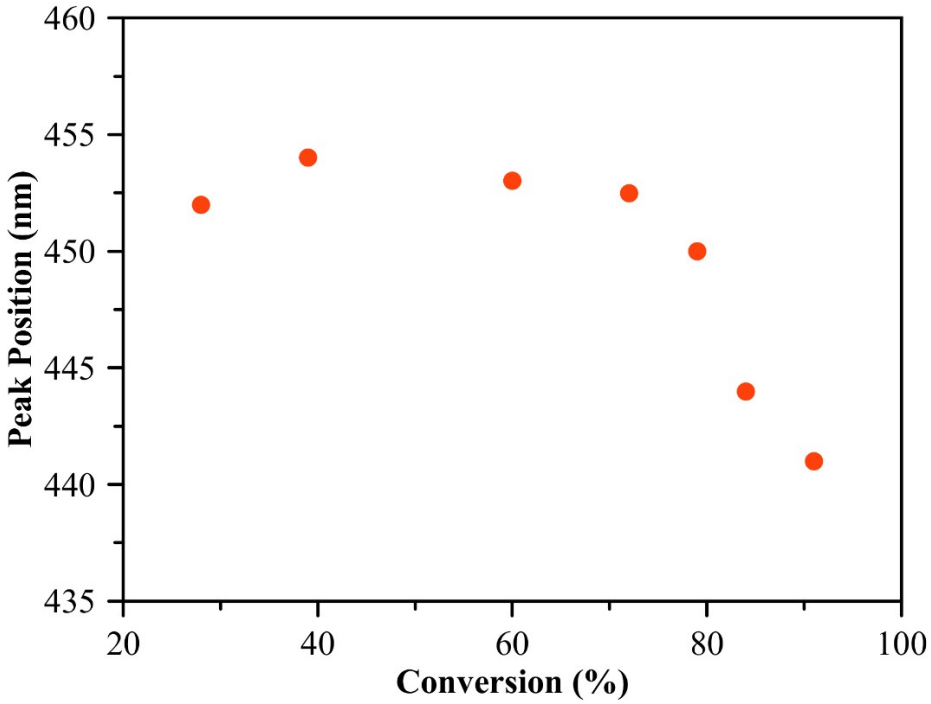

Fig. S13b. Extinction peak position in the 440-460 nm region of the UV-Vis extinction spectrum as a function of PA conversion for SCR between PA and iodobenzene (IB) in the presence of base.

Fig. S13b shows that during the SCR between PA and IB, the peak position changes in the range of ~440-455 nm. We also observed that the maximum range of change in peak position depends on the aryl-halide (Ar-X) coupling partner. For example, when nitro-Iodobenzene is used as coupling partner, we observed the change in the peak position in the range of 440 to 481 nm. These results indicate that the homogeneous Cu species formed via PA-induced leaching of surface atoms further interact with the aryl-halide partner to form other

homogeneous Cu species in the catalytic cycle. The extinction peaks of these Cu catalytic species are closely spaced, their combined extinction peaks appear as a single peak in the measured UV-Vis extinction spectrum. The results also suggest that the changes observed in the measured extinction peak position are due to the change in the relative concentration of these homogeneous Cu catalytic species with reaction time and conversion.

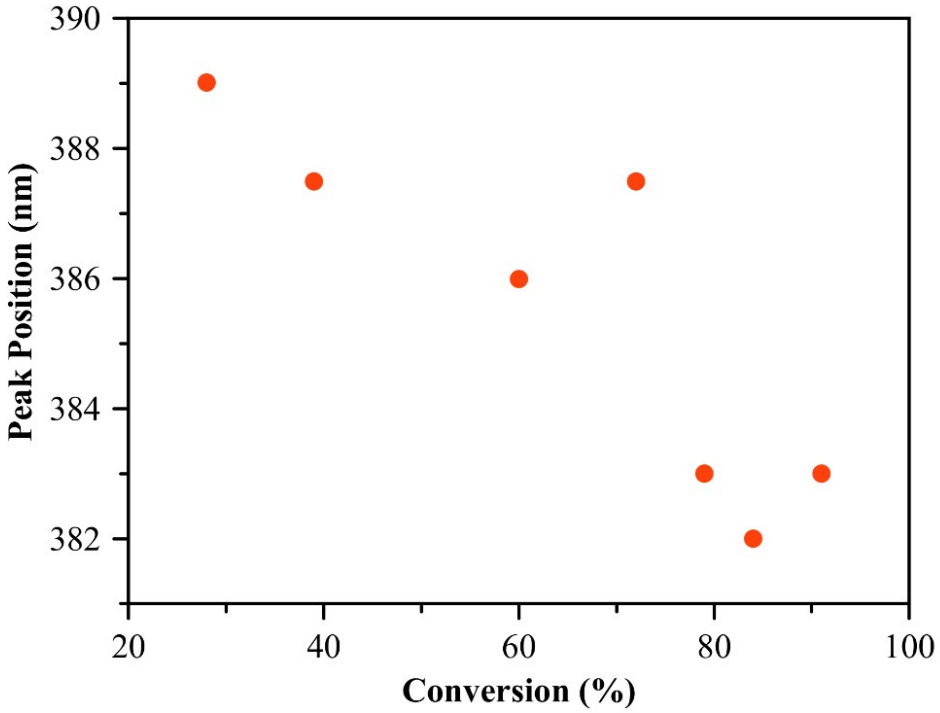

Fig. S13c. Extinction peak position in the 380-390 nm region of the UV-Vis extinction spectrum as a function of PA conversion for SCR in the presence of base.

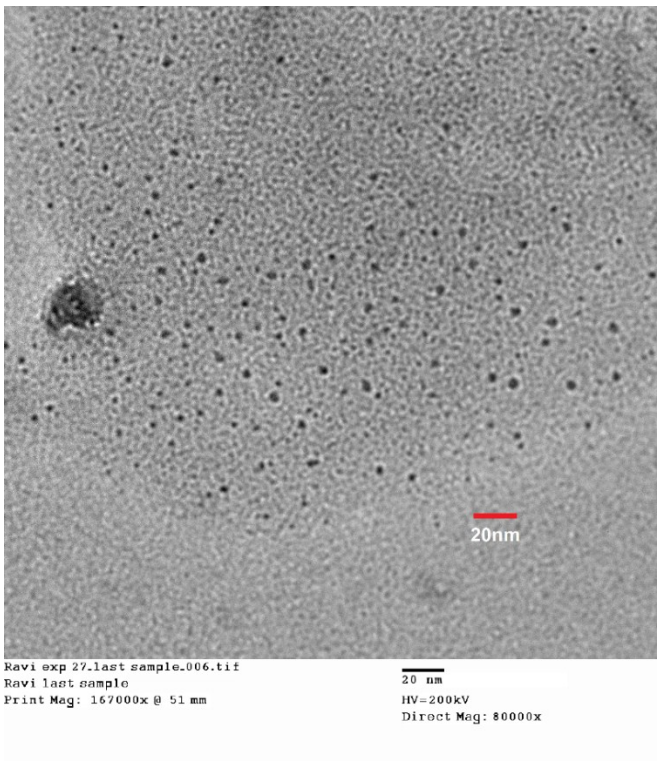

Fig. S14a. Representative TEM image of blacked out nanoclusters (average size: 3 ± 0.7 nm) observed in the reaction solution at the end of OHR.

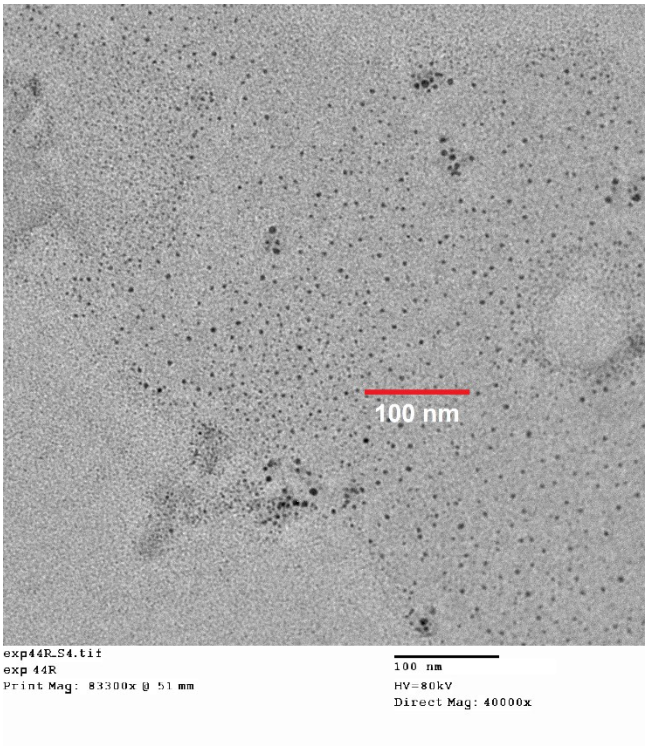

Fig. S14b. Representative TEM image of blacked out nanoclusters (average size: 3.6 ± 0.94 nm) observed in the reaction solution at the end of SCR.

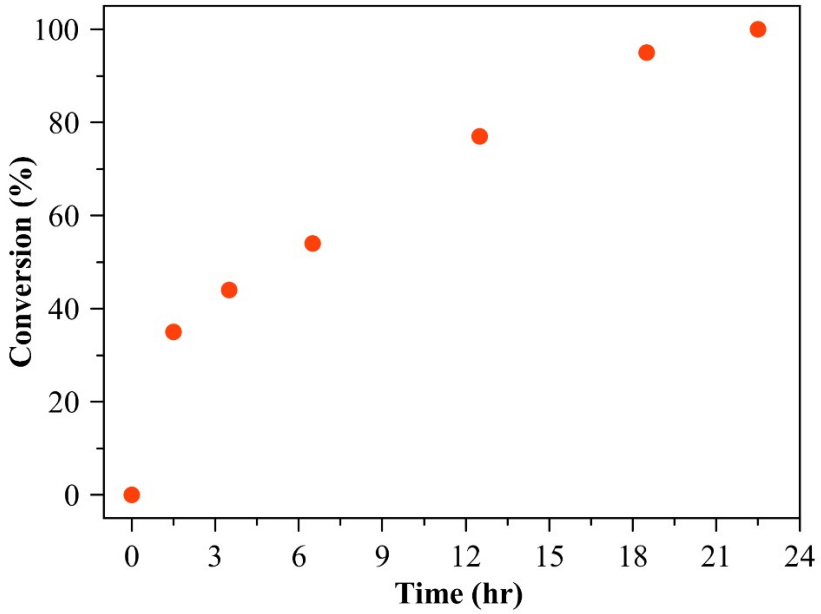

Fig. S15. Conversion as a function of Reaction Time for SCR between PA and bromobenzene at 147 °C (under reflux) in the presence of the base.

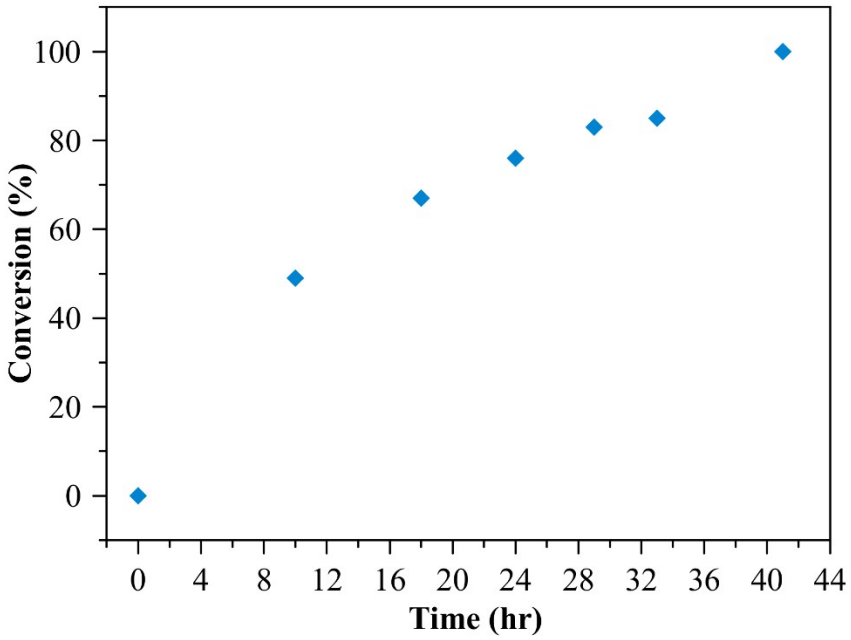

Fig. S16. Conversion as a function of Reaction Time for SCR between PA and bromoenzene at 147 °C (under reflux) in the absence of the base.

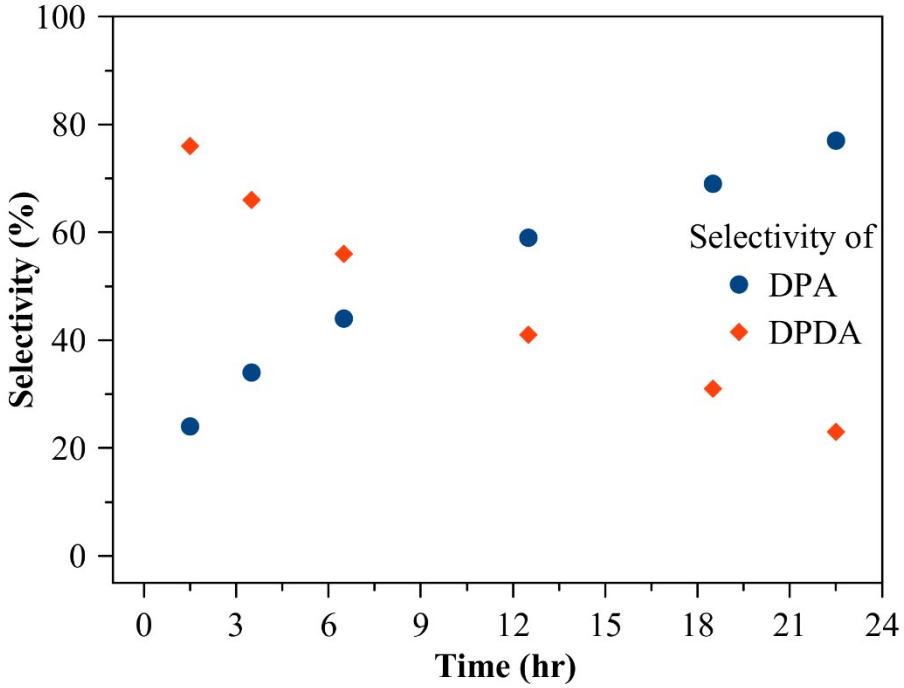

Fig. S17. The cross-coupling and homocoupling products DPA vs DPDA selectivity as a function of reaction time for SCR between PA and bromobenzene at 147 °C (under reflux) in the presence of the base.

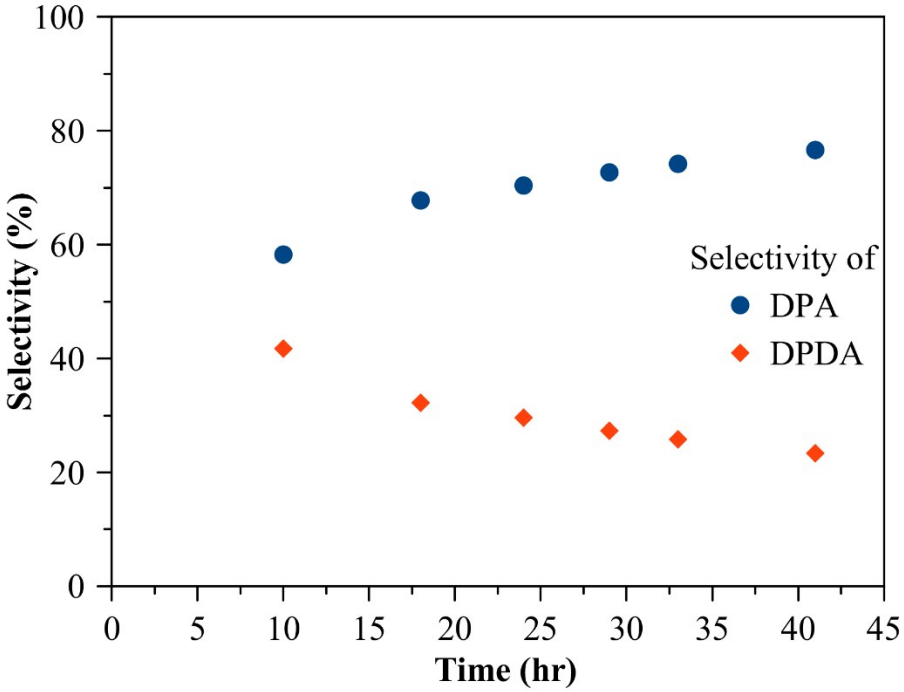

Fig. S18. The cross-coupling and homocoupling products DPA vs DPDA selectivity as a function of reaction time for SCR between PA and bromobenzene at 147 °C (under reflux) in the absence of the base.

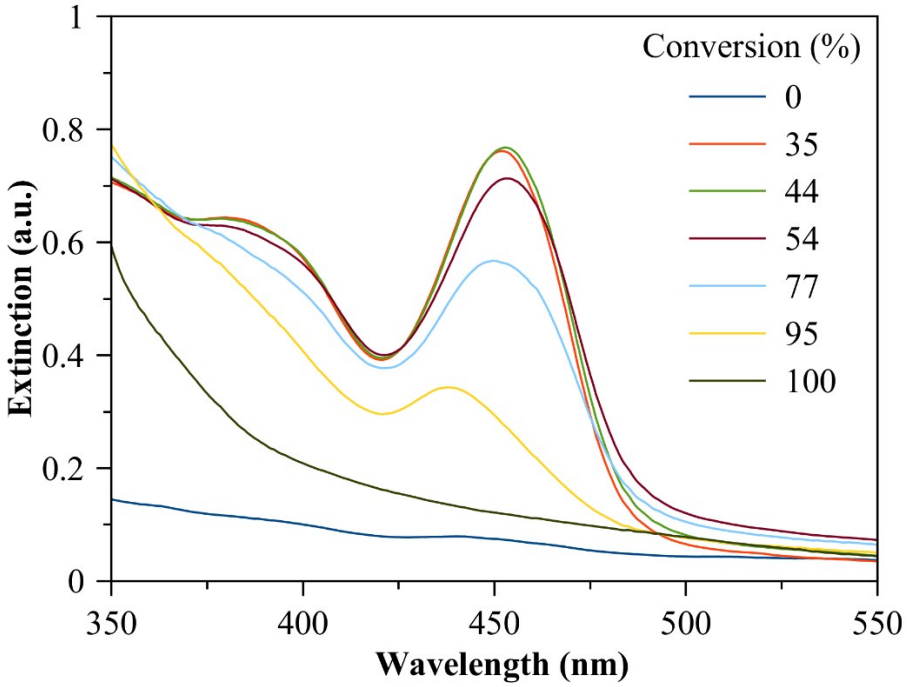

Fig. S19. UV-Vis extinction spectra of reaction mixture measured at different reaction conversions during SCR between PA and bromobenzene at 147 °C (under reflux) in the presence of base. The extinction peaks centered at ~385 and ~450 nm in Fig. S8 are due to homogeneous Cu complexes in the reaction solution. These peaks are observed in the reaction solution only when both PA and base are present.

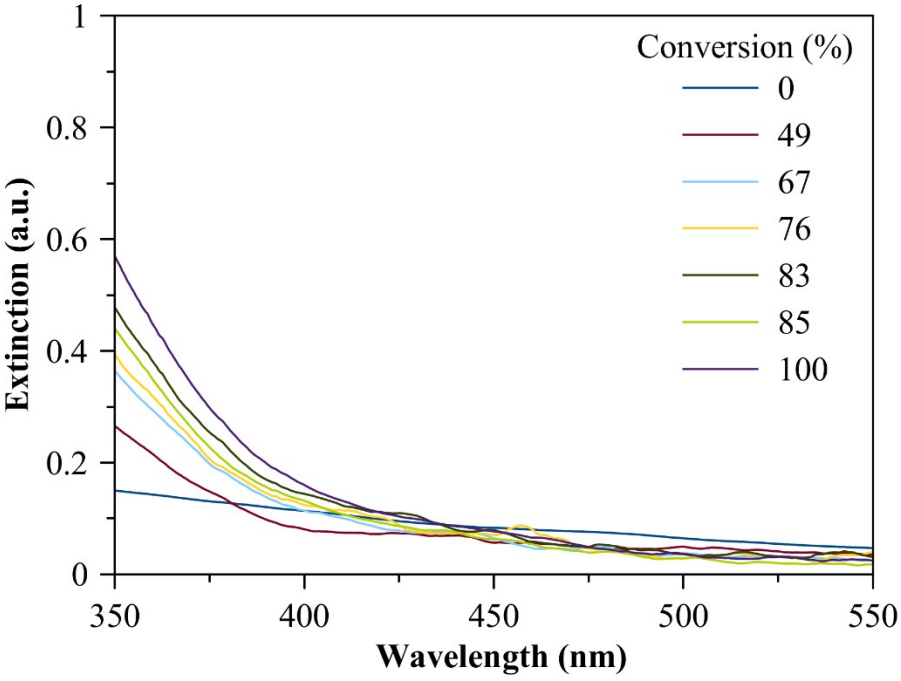

Fig. S20. UV-Vis extinction spectra of reaction mixture measured at different reaction conversions during SCR with Bromo Benzene at 147 °C (under reflux) in the absence of the base. The changes observed in the extinction spectra in Fig. S19 for different conversions are most likely due to the expected change in dielectric constant of the reaction mixture for the respective conversions.

Reference Cited for Electronic Supplementary Information

1 A. Marimuthu, J. Zhang and S. Linic, *Science*, 2013, **339**, 1590–1593.
2 G. Kresse and J. Furthmüller, *Phys. Rev. B*, 1996, **54**, 11169–11186.
3 P. E. Blöchl, *Phys. Rev. B*, 1994, **50**, 17953–17979.
4 J. P. Perdew, K. Burke and M. Ernzerhof, *Phys. Rev. Lett.*, 1996, **77**, 3865–3868.
5 S. Grimme, J. Antony, S. Ehrlich and H. Krieg, *J. Chem. Phys.*, 2010, **132**, 154104.
6 S. Grimme, S. Ehrlich and L. Goerigk, *J Comput Chem*, 2011, **32**, 1456–1465.
7 K. Mathew, R. Sundararaman, K. Letchworth-Weaver, T. A. Arias and R. G. Hennig, *J. Chem. Phys.*, 2014, **140**, 084106.
8 M. Fishman, H. L. Zhuang, K. Mathew, W. Dirschka and R. G. Hennig, *Phys. Rev. B*, 2013, **87**, 245402.
9 M. Gajdoš, K. Hummer, G. Kresse, J. Furthmüller and F. Bechstedt, *Phys. Rev. B*, 2006, **73**, 045112.
10 Isotope Distribution Calculator and Mass Spec Plotter., https://www.sisweb.com/mstools/isotope.htm, (accessed September 29, 2016).
11 Phenylethyne, https://webbook.nist.gov/cgi/cbook.cgi?ID=536-74-3, (accessed May 4, 2019).
12 Benzene, iodo-, https://webbook.nist.gov/cgi/cbook.cgi?ID=C591504&Mask=400, (accessed May 4, 2019).
13 Diphenylacetylene, https://webbook.nist.gov/cgi/cbook.cgi?ID=C501655&Mask=400, (accessed May 4, 2019).

